HHS Public Access

Author manuscript

*Retina*. Author manuscript; available in PMC 2022 February 01.

Published in final edited form as:

*Retina*. 2021 February 01; 41(2): 381–386. doi:10.1097/IAE.0000000000002875.

# The Fingerprint Sign of the Henle Fiber Layer

**Shane M. Griffin, BA**[1], **H. Richard McDonald, MD**[2,4], **Robert N. Johnson, MD**[2,4], **J. Michael Jumper, MD**[2,4], **Arthur D. Fu, MD**[2,4], **Emmett T. Cunningham Jr, MD, PhD, MPH**[2,3,4,5], **Kiang Lee, MD, PhD**[1], **Caleb C. Ng, MD**[2,4], **Brandon J. Lujan, MD**[1,2]

[1]Casey Eye Institute, Oregon Health & Science University, Portland, OR

[2]West Coast Retina Medical Group, San Francisco, CA

[3]Department of Ophthalmology, Stanford University School of Medicine, Stanford, CA

[4]Department of Ophthalmology, California Pacific Medical Center, San Francisco, CA

[5]The Francis I Proctor Foundation, UCSF School of Medicine, San Francisco, CA

## Abstract

**Purpose:** To describe the appearance of concentric, fingerprint-like waves within the Henle Fiber Layer (HFL) using *en face* optical coherence tomography (OCT) in patients with tractional pathologies of the retina.

**Methods:** Retrospective analysis of 6 eyes of 6 patients imaged by OCT with volumetric slabs positioned at the level of the HFL.

**Results:** OCT data from 6 patients with tractional vitreoretinal pathology were reviewed. Concentric, fingerprint-like microwaves were visualized via *en face* OCT in all 6 study eyes at the level of the HFL. This finding resembled the finding of HFL waves previously noted histopathologically from force exerted on this layer.

**Conclusion:** In retinal pathologies in which specific physical forces act upon the retina, volumetric OCT may permit visualization of *en face* concentric, fingerprint-like hyper-reflective rings within the HFL. This “fingerprint sign” may represent a biomechanical consequence of traction on the retina and allow clinical decision-making based on improved recognition of the existence of such traction.

**Summary Statement:** Concentric hyper-reflective rings visualized by *en face* optical coherence tomography in patients with tractional pathologies of the retina may be caused by physical waves within the Henle Fiber Layer.

### Keywords

Concentric Waves; Directional OCT; *En Face OCT*; Epiretinal Membrane; Foveal Hypoplasia; Henle Fiber Layer; Müller cell; Outer Nuclear Layer; Outer Plexiform Layer; Volumetric imaging

**Corresponding Author Name** Brandon J. Lujan, Casey Eye Institute, 515 SW Campus Dr. Portland, OR, 97239. lujanb@ohsu.edu.

## Introduction

The Henle Fiber Layer (HFL) is comprised of Müller cells and parallel photoreceptor axons projecting radially toward the synaptic outer plexiform layer (OPL) [1,2] They may distend in tractional retinopathies and divide the outer nuclear layer (ONL) from the remaining OPL.[2,3] The oblique path of the HFL grants unique structural and reflectance properties. Behaving as a layer of centrifugal cylinders, HFL reflectivity varies as a function of the incident angle of light, with maximal reflectance occurring when light is oriented perpendicular to its fibers.[4]

Alterations in the orientation of the HFL change its reflectivity profile, and these changes may be visualized *in vivo* via optical coherence tomography (OCT).[4] Distortion of the HFL gives rise to cross-sectional OCT imaging findings, for example: hyper-reflective HFL overlying drusen.[4] Related to the varying reflectance patterns of the HFL, the cross-sectional OCT appearances of the OPL/HFL interface have previously been classified: bright, columnar, dentate, delimited, indistinct, or dark.[5] Here, we use *en face* OCT to study a series of patients with a dentate, or tooth-like, appearance of the OPL/HFL interface on cross-sectional OCT. The use of volumetric imaging and analysis gives rise to an *en face* OCT finding: concentric waves within the HFL centered on the fovea. This study characterizes *en face* OCT concentric waves within the HFL seen in tractional vitreoretinal pathology. Furthermore, we provide an explanation of this finding based on previously published histological evidence and imaging findings. Finally, we explore the implications of this *en face* finding as well as propose applications for use of the “fingerprint sign” in clinical practice.

## Methods

Our observational imaging study was approved by the Western Institutional Review Board (IRB), image analysis was approved by the Oregon Health & Science University IRB, and all procedures conformed to the Declaration of Helsinki. Participants were identified by chart review including review of previous Cirrus HD-OCT spectral domain OCT (SD-OCT) scans consisting of macular frame-averaged horizontal cross-sectional and Macular Cube 512×128 scans. Cirrus Advanced Visualization software was utilized to generate RPE-contoured slabs of thicknesses between 31–47 microns, which were positioned in order to optimally encompass the HFL. Contrast and brightness of the images were manually adjusted to enhance visualization of the *en face* concentric rings.

## Results

Six eyes of six subjects were identified by chart review. These 4 male and 2 female subjects had a median age of 68 (Range: 54–80) and visual acuities ranging from 20/32 to 20/400 upon initial presentation with tractional retinal pathologies. Underlying systemic co-morbidities included: hypertension, erectile dysfunction treated with sildenafil, hypercholesterolemia, basal cell carcinoma, allergic rhinitis, asthma, osteoarthritis, ischemic stroke, and atrial fibrillation. Ocular comorbidities included: macular degeneration, central serous chorioretinopathy (CSCR), retinal tear, myelinated nerve fiber, high myopia, choroidal nevus, and pseudophakia. In these 6 cases, an ERM was visualized as a thickened

hyper-reflective linear structure present internal to the level of the ILM on horizontal B-scan (Figure 1C). In each of the cases presented, cross-sectional B-scans uniformly showed a tooth-like pattern at the OPL/HFL interface (Figure 1C). In one representative case (Figure 1), color fundus photography, fluorescein angiography, and infrared imaging were normal with only a hint of a circular pattern visualized. However, *en face* analysis through the HFL showed the appearance of concentric hyper- and hypo-reflective waves (Figure 1A-B). This same pattern was visualized in the other subjects with ERM (Figure 2). Although, the appearance of HFL waves was similar in each of the 6 cases presented, the lateral extent of this pattern varied between patients, as did the frequency and spacing between ridges (Figure 2). Short case vignettes follow and are summarized in Table 1.

**Case 1.**

A 71-year-old man presented with 1–2 months of blurred vision bilaterally. His visual acuities were 20/20 OD and 20/40 OS. Examination was notable for ERM with macular pseudohole OS. Following tentative diagnosis of ARMD OU and ERM OS a plan for further observation was made. The left eye, the study eye, exhibited the *en face* finding and was imaged at this baseline visit.

**Case 2.**

A 64-year-old man presented with 2–3 weeks of decreased central vision in his left eye. At this initial visit his visual acuities were 20/63 OD and 20/63 OS. His examination was notable for an ERM OD and subfoveal subretinal fluid (SRF) OS. A diagnosis of CSCR OS and ERM OD was made with an initial plan for observation. The right eye, the study eye, exhibited the *en face* finding and was imaged at this baseline visit. The subfoveal SRF OS persisted upon multiple follow up exams but had resolved by 8 months after his initial presentation.

**Case 3.**

A 65-year-old man presented with blurred central vision OD. His visual acuities were 20/80 OD and 20/32 OS. Examination was significant for posterior vitreous detachment (PVD), ERM, and nasal myelinated nerve fiber OD. Referral was made for surgical evaluation of ERM OD, but the patient initially elected observation. The right eye, the study eye, exhibited the *en face* finding and was imaged at this visit. 6 months following initial presentation, worsening distortion of his vision OD prompted the patient to elect surgery and ERM and ILM peeling was subsequently performed. 3 months following surgery, visual acuity had improved to 20/40 OS. The patient subsequently underwent cataract extraction with intraocular lens placement (CEIOL) OD. Vision remained stable at 20/25 OD and 20/20–2 OS 5 years following his initial presentation.

**Case 4.**

A 72-year-old woman presented 10 months after repair of a traumatic macular hole in her right eye. Her visual acuities were 20/50 OD, and 20/20 OS. Examination was notable for PCIOL, trace ERM, and closed macular hole OD. Initially, the plan for her ERM in the right eye was observation. The right eye, the study eye, exhibited the *en face* finding and was

imaged at this visit. Annual follow-up exams have remained mostly unremarkable with stable vision OU more than 5 years after initial presentation.

### Case 5.

An 80-year-old woman presented with visual distortion OS. Visual acuities were 20/20 OD and 20/32 OS. Examination was significant for bilateral ERMs (OS>OD), intraocular implant lens OU, and PVD OD. No *en face* finding was evident in either eye at this time. Surgical repair of the ERM OS was performed. Six months following surgery, the patient was 20/32 ph 20/20 OD and 20/20 OS and reported visual distortion in the right eye. The patient elected PPV with membranectomy in the right eye. Pre-operatively, the right eye, the study eye, exhibited the *en face* finding and was imaged. Post-operatively vision improved to 20/20 OU and remained stable.

### Case 6.

A 54-year-old man presented reporting a trapezoidal scotoma following PPV with membranectomy, gas fluid exchange, and laser OD performed to treat his macular hole. He had a previous history of retinal tear OD treated with laser barricade and cryopexy as well as a retinal tear OS previously treated with laser barricade. Upon presentation following repair of his macular hole OD, his visual acuities were 20/400 OD and 20/13 OS. At that time, examination was notable for an ERM OD. The right eye, the study eye, exhibited the *en face* finding and was imaged at this visit. Refracting to 20/80 with −6.5 D 2 months post-operatively, the patient continued to report a trapezoidal scotoma. Following cataract surgery, the patient's vision further improved to 20/40 OD. However, his "parallelogram-shaped" scotoma in the right eye persisted. Following YAG capsulotomy 4 months after his cataract surgery, there was a persistent geometric scotoma just inferior to center consistent with photoreceptor disruption in this area. The patient's vision remained stable at 20/40 OD 1 year following initial visit for ERM.

## Discussion

Volumetric SD-OCT imaging permits three-dimensional visualization of micro-architectural alterations within specific retinal layers. Our study demonstrates concentric hyper- and hypo-reflective waves within the HFL visualized via *en face* OCT, resembling a fingerprint centered on the fovea. This finding adds a three-dimensional representation of the HFL to cross-sectional OCT images demonstrating a tooth-like pattern at the OPL/HFL interface.[5] We hypothesize a model to explain the observed *en face* concentric waves: they result from anteroposterior undulations of the photoreceptor axons and Müller cell processes within the HFL. In this model, the hyper-reflective crests of concentric waves represent the peak and trough positions where fibrillar orientation approaches perpendicular to light emitted from and reflected directly back to the OCT system. In contrast, light incident on the HFL where its fibers are more parallel is reflected away from the OCT detector. These regions within the HFL are therefore hypo-reflective. Along each group of Henle fibers radiating from the foveal center, waves within its substance would therefore account for alternating periodic reflectivity and generate an *en face* ripple appearance (Figure 2).

Our report may help to explain previous reports of concentric macular rings. Using infrared reflectance (IRR), patients with foveal hypoplasia exhibit the “concentric macular ring sign” (CMR)[6] and *en face* concentric rings have been identified in the maculae of subjects with albinism.[7] Similar to the those presented here, in these previous reports a tooth-like appearance was seen in corresponding B-scans at the OPL/HFL interface with *en face* concentric waves visualized when the volumetric OCT slab was positioned at the depth of the HFL (Figure 1B).[7] The unique physical properties of the cells composing the HFL may explain this *en face* concentric wave pattern.

Wolter histologically identified waves within the HFL in a case of compression of the retina by an orbital tumor (Figure 3). In this case, pressure on the globe caused horizontal folding of the inner retinal layers, Bruch’s membrane, and the choroid. Distinct from the ocular changes seen elsewhere, concentric “microwaves” were identified within the HFL.[8] We posit that HFL waves represent a directional response of clustered fibers as force is transferred through axons and Müller cells. Axonal morphological characteristics include an elastic response to stretch and a wavy appearance following the release of tension (Figure 3).[9] Compression of the retina by a malignant mass gave rise to Wolter’s histological finding and may similarly help to explain the “shark-teeth” sign seen in combined hamartoma of the retina and retinal pigment epithelium (CHRRPE).[10]

Anisotropic cellular responses to the disruption of retinal architecture may explain concentric *en face* waves. Acting like springs, Müller cells contribute to the structural integrity of the retina during development and under mechanical stress.[11] Functioning as mechanoreceptors, these cells alter protein expression in response to directional forces in the retina.[12] In the formation of ERMs, fibrosis is driven by Müller cells being stimulated by cytokines.[13] Elaboration of extracellular matrix (ECM) proteins, including collagens, leads to progressive contraction of the retina.[13] As key mediators of ERM formation, Müller cells are likely contributors to the formation of HFL waves. As an ERM tugs the inner retina, “accordion contraction” has previously been reported at the OPL/HFL interface.[3] This explanation for *en face* HFL waves is consistent with known responses of the cellular processes composing the HFL under physical force. The resulting reflectance pattern is similarly corroborated by previous OCT studies.

OCT images of crimped collagenous tissues, ligaments and tendons from rodent tails, under mechanical stress show periodic alternating hyper- and hyporeflective segments within fibrils.[14] Comparable to the HFL appearance demonstrated in this study, a similar reflectance pattern has been observed in the lamina cribrosa, where waviness, crimp, diminishes as the force exerted upon its collagen fibrils increases.[15] The degree of crimp in these fibers may be quantified by summing adjacent lengths of bright and dark segments to measure the wavelength of these fibrils.[15] As crimp measurements in the lamina cribrosa explain how the eye adapts to intraocular pressure (IOP) fluctuations, analyzing *en face* HFL waves may help to explain how the retina reacts to physical stress as well.

Understanding how the retina responds to mechanical forces may inform treatment decisions for patients with ERM. Commonly experienced by these patients including *Cases 3 & 5*, metamorphopsia is directly related to structural contraction of the retina.[16] Müller cell

reorientation during traction may help to explain metamorphopsia as well as macropsia, a distinctive visual manifestation of the retina under traction.[17] As Müller cells transfer force to photoreceptors in the central foveal bouquet, imaging findings indicating that Müller cell disruption has occurred could have predictive visual significance for patients.[18] In ERM patients with or without metamorphopsia, the presence of *en face* concentric waves may relate to visual outcomes and could provide prognostic information regarding the potential for recovery following treatment. Specifically, the presence of *en face* concentric waves and the period of waves in the HFL could potentially serve as useful measures of retinal traction during surgery.

Identification of *en face* concentric waves in foveal hypoplasia demands further investigation.[7] The potential mechanisms of its presence in this very different pathological condition remain to be elucidated. The presence of the fingerprint sign should not be limited to vitreoretinal tractional pathology, and hypothetically could be found in a variety of conditions where force is exerted on the HFL, such as in the subject identified microscopically by Wolter.

Our hypothesis that physical waves within the HFL cause the reported *en face* finding cannot be proven due to the observational nature of our report. This limitation should spur future investigation suited to test this hypothesis with larger samples of subjects with ERM, macular hole, foveal hypoplasia, and other retinal pathologies discussed herein. Additional anatomical evaluations including retinal layer thickness and foveal displacement, and functional evaluations including microperimetry will be important correlations to explore in future prospective studies. Future research could also assess the prognostic value of identifying *en face* concentric HFL waves in patients. At the time that these images were collected, we were limited by the absence of commercially-available segmentation software capable of mirroring the HFL posterior to the OPL, so an RPE-contoured slab was instead utilized. However, research segmentation software capable of obtaining these HFL slabs is now available. These tools may allow for a more robust and quantitative means of measuring the extent of waves in HFL as well as the HFL wave period in diverse clinical scenarios.

## Acknowledgements:

Supported by grant P30 EY010572 from National Institutes of Health (Bethesda, MD), and by unrestricted departmental funding from Research to Prevent Blindness (New York, NY).

Authors thank Austin Roorda for his optical expertise

Funding Sources:

*None of the authors have proprietary interests related to this study.

## References

1. Curcio CA, Allen KA. Topography of ganglion cells in human retina. J Comp Neurol. 1990;300(1):5–25. doi:10.1002/cne.903000103 [PubMed: 2229487]
2. Govetto A, Hubschman J-P, Sarraf D, et al. The role of Müller cells in tractional macular disorders: an optical coherence tomography study and physical model of mechanical force transmission. Br J Ophthalmol. 2019:bjophthalmol-2019–314245. doi:10.1136/bjophthalmol-2019-314245

3. Pang CE, Spaide RF, Freund KB. Epiretinal proliferation seen in association with lamellar macular holes: A distinct clinical entity. Retina. 2014;34(8):1513–1523. doi:10.1097/IAE.0000000000000163 [PubMed: 24732699]
4. Lujan BJ, Roorda A, Knighton RW, Carroll J. Revealing Henle's fiber layer using spectral domain optical coherence tomography. Investig Ophthalmol Vis Sci. 2011;52(3):1486–1492. doi:10.1167/iovs.10-5946 [PubMed: 21071737]
5. Ouyang Y, Walsh AC, Keane PA, et al. Different phenotypes of the appearance of the outer plexiform layer on optical coherence tomography. Graefe's Arch Clin Exp Ophthalmol. 2013;251(10):2311–2317. doi:10.1007/s00417-013-2308-5 [PubMed: 23661097]
6. Cornish KS, Reddy AR, McBain VA. Concentric macular rings sign in patients with foveal hypoplasia. JAMA Ophthalmol. 2014;132(9):1084–1088. doi:10.1001/jamaophthalmol.2014.1715 [PubMed: 24945710]
7. Lee DJ, Woertz EN, Visotcky A, et al. The henle fiber layer in albinism: Comparison to normal and relationship to outer nuclear layer thickness and foveal cone density. Investig Ophthalmol Vis Sci. 2018;59(13):5336–5348. doi:10.1167/iovs.18-24145 [PubMed: 30398625]
8. Wolter JR. Concentric "microwaves" of Henle's fiber layer: Associated with horizontal folding. Albr von Graefe's Arch Clin Exp Ophthalmol. 1981;216(1):31–39. doi:10.1007/BF00407774
9. Van Essen DC. A tension-based theory of morphogenesis and compact wiring in the central nervous system. Nature. 1997;385(6614):313–318. doi:10.1038/385313a0 [PubMed: 9002514]
10. Arrigo A, Corbelli E, Aragona E, et al. Optical Coherence Tomography and Optical Coherence Tomography Angiography Evaluation of Combined Hamartoma of the Retina and Retinal Pigment Epithelium. Retina. 2019;39(5):1009–1015. doi:10.1097/IAE.0000000000002053 [PubMed: 29370036]
11. MacDonald RB, Randlett O, Oswald J, et al. Müller glia provide essential tensile strength to the developing retina. J Cell Biol. 2015;210(7):1075–1083. doi:10.1083/jcb.201503115 [PubMed: 26416961]
12. Vecino E, Rodriguez FD, Ruzafa N, et al. Glia-neuron interactions in the mammalian retina. Prog Retin Eye Res. 2016;51:1–40. doi:10.1016/j.preteyeres.2015.06.003 [PubMed: 26113209]
13. Kanda A, Noda K, Hirose I, Ishida S. TGF-β-SNAIL axis induces Müller glial-mesenchymal transition in the pathogenesis of idiopathic epiretinal membrane. Sci Rep. 2019;9(1):1–13. doi:10.1038/s41598-018-36917-9 [PubMed: 30626917]
14. Hansen KA, Weiss JA, Barton JK. Recruitment of tendon crimp with applied tensile strain. J Biomech Eng. 2002;124(1):72–77. doi:10.1115/1.1427698 [PubMed: 11871607]
15. Jan NJ, Gomez C, Moed S, et al. Microstructural crimp of the lamina cribrosa and peripapillary sclera collagen fibers. Investig Ophthalmol Vis Sci. 2017;58(9):3378–3388. doi:10.1167/iovs.17-21811 [PubMed: 28687851]
16. Nomoto H, Matsumoto C, Arimura E, et al. Quantification of changes in metamorphopsia and retinal contraction in eyes with spontaneous separation of idiopathic epiretinal membrane. Eye. 2013;27(8):924–930. doi:10.1038/eye.2013.108 [PubMed: 23722721]
17. Colakoglu A, Akar SB. Potential role of Müller cells in the pathogenesis of macropsia associated with epiretinal membrane: A hypothesis revisited. Int J Ophthalmol. 2017;10(11):1759–1767. doi:10.18240/ijo.2017.11.19 [PubMed: 29181322]
18. Govetto A, Bhavsar KV, Virgili G, et al. Tractional Abnormalities of the Central Foveal Bouquet in Epiretinal Membranes: Clinical Spectrum and Pathophysiological Perspectives. Am J Ophthalmol. 2017;184:167–180. doi:10.1016/j.ajo.2017.10.011 [PubMed: 29106913]

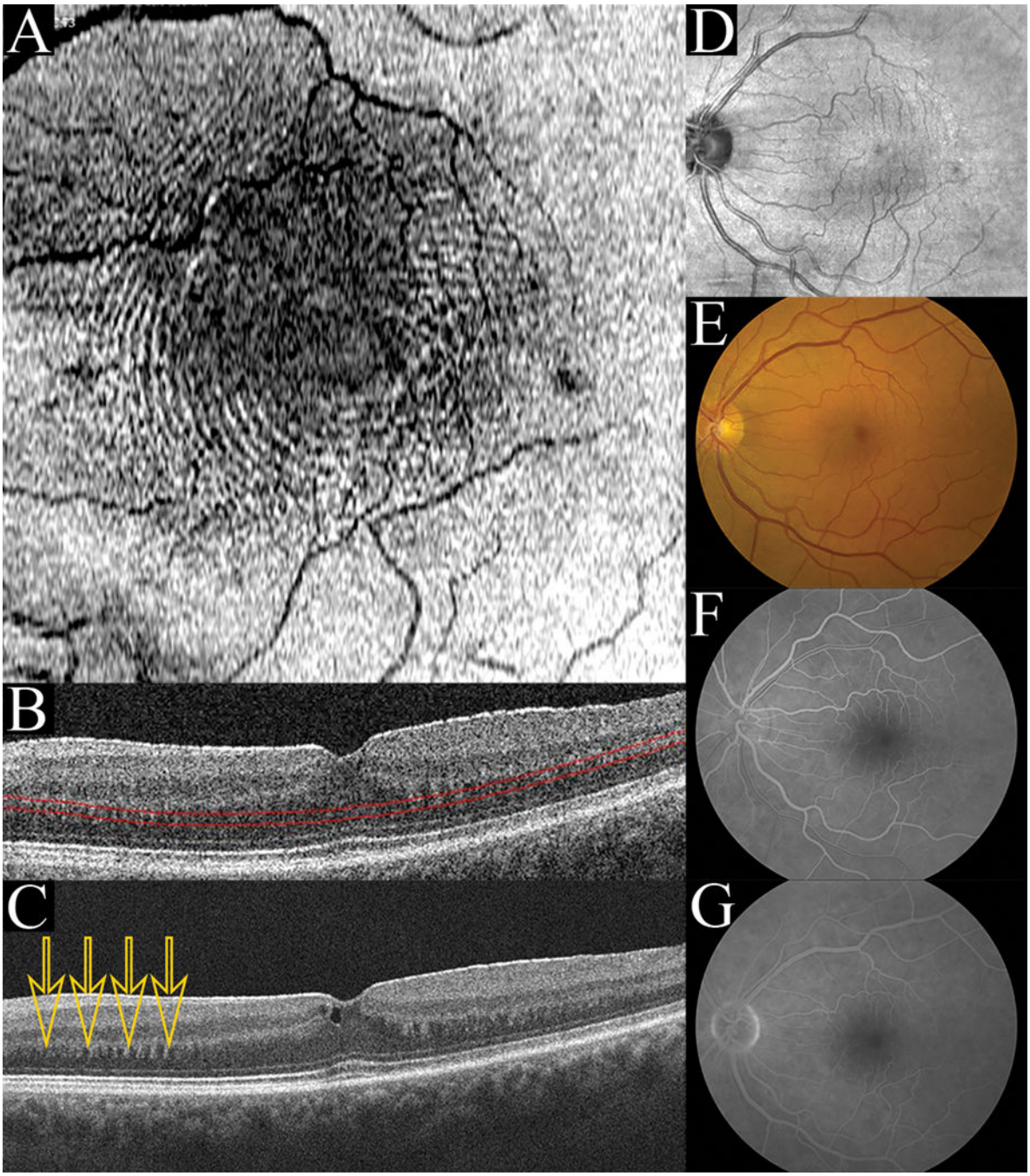


**Figure 1:**

**(*Case* 1)**: En face concentric waves (A) are seen when a contoured slab is positioned at the level of the HFL (B). Averaged B-scan through the fovea (C) reveals a dentate appearance of the synaptic OPL/HFL junction (arrows) and a hyper-reflective ERM is seen. Infrared imaging (D), Fundus photography (E), early fluorescein angiography (F), and late fluorescein angiography (G) do not show the concentric wave pattern.

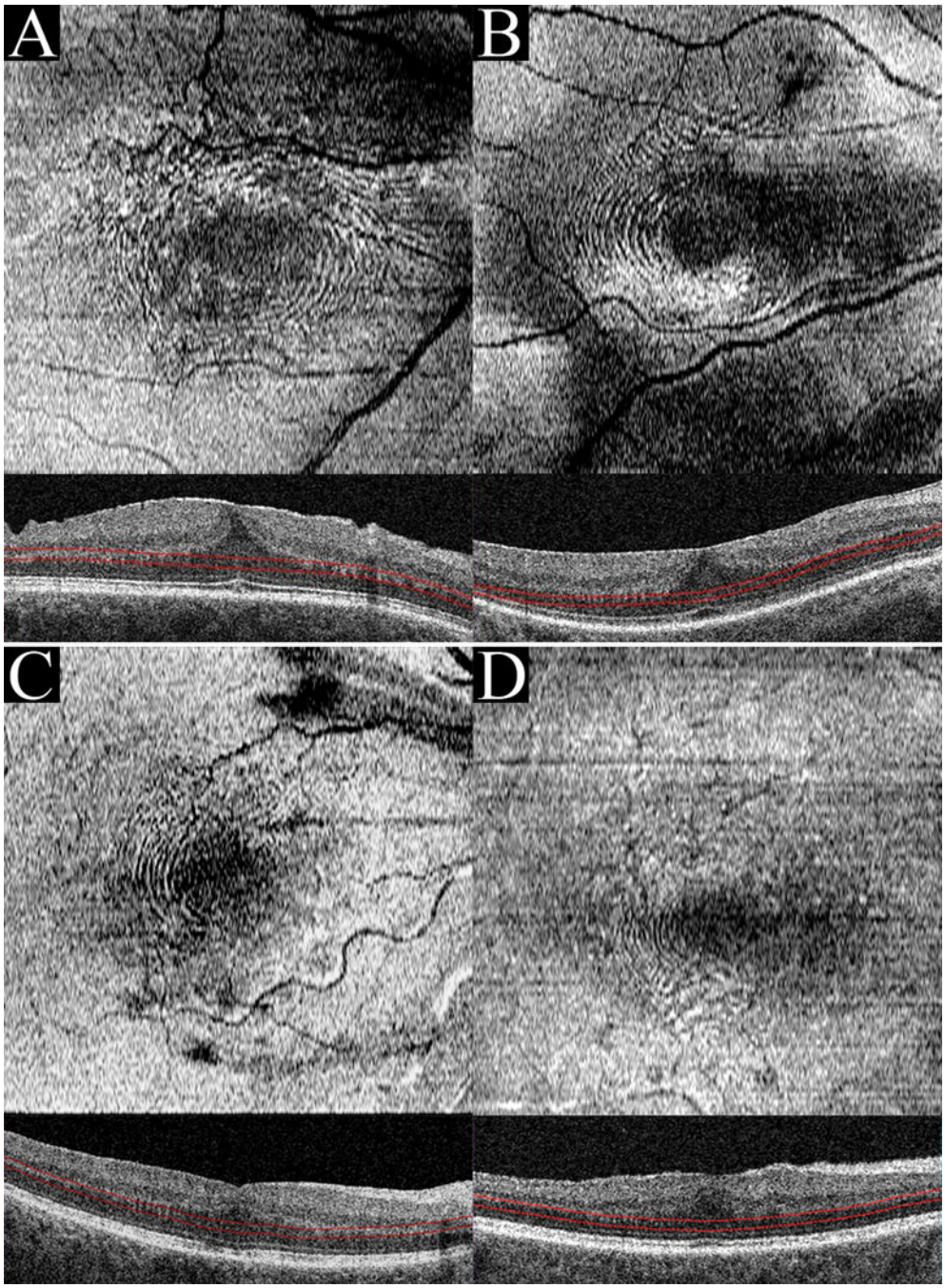


**Figure 2:**
When RPE-contoured slabs of thickness between 31–47 microns were positioned at the level of the HFL, the *en face* "fingerprint sign" was visualized. Case 2(A), Case 3(B), Case 4(C), and Case 5(D) all presented with ERM.

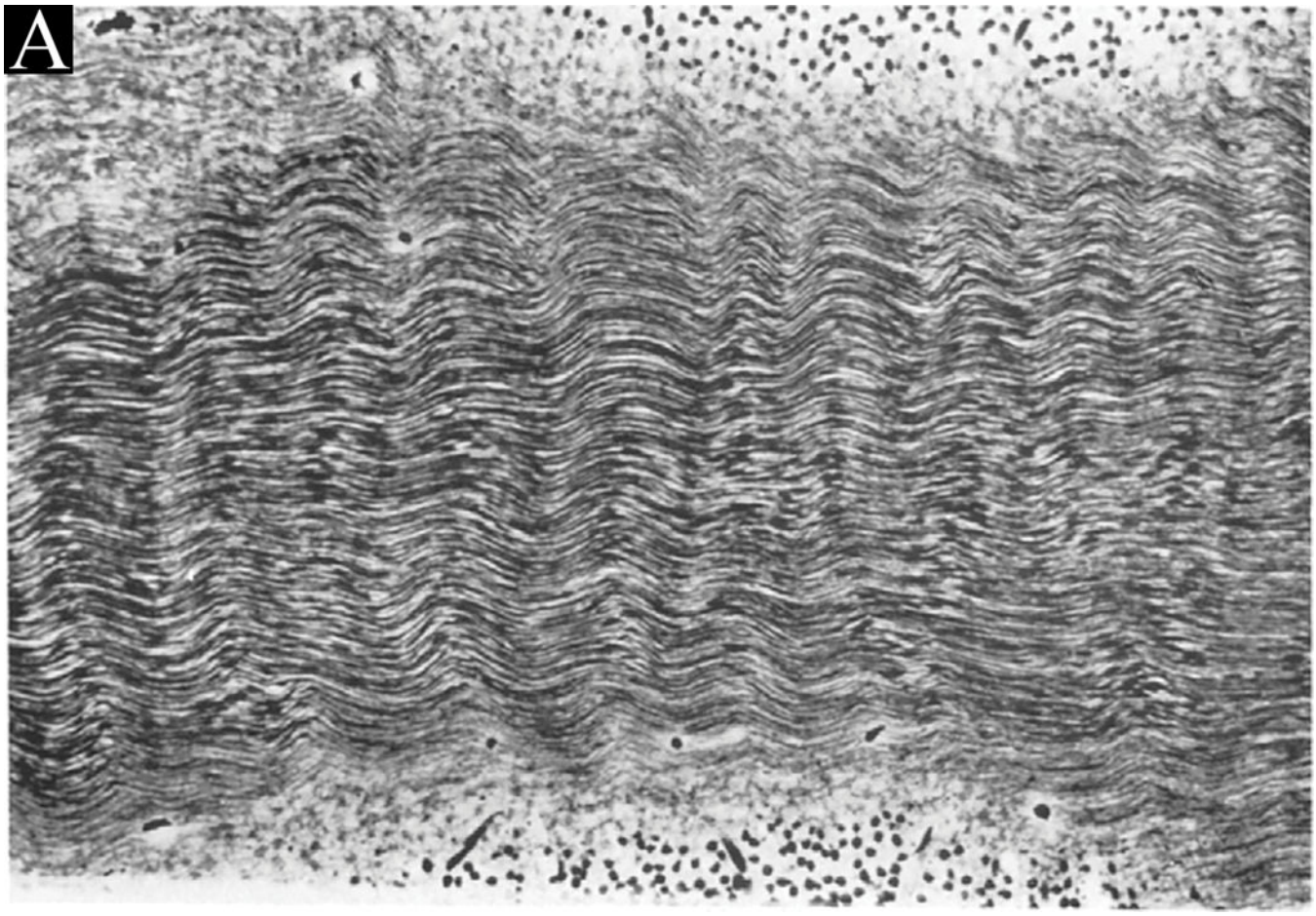


**Figure 3:**
Wolter's histological photographs demonstrating physical waves within the HFL. "Fig. 4. (Wolter) A part of the temporal aspect of Henle's fiber layer exhibiting regular 'microwaves' with ridges and valleys in a vertical direction. All fibers are well preserved. Flat frozen section, Hortega stain, photomicrograph × 300"

**Table 1:**

Case summaries.

| Case | Age | Sex | Eye | VA | Diagnosis |
|---|---|---|---|---|---|
| 1 | 71 | M | OS | 20/40 | ERM with pseudohole |
| 2 | 64 | M | OD | 20/63 | ERM |
| 3 | 65 | M | OD | 20/80 | ERM |
| 4 | 72 | F | OD | 20/50 | ERM following macular hole repair |
| 5 | 80 | F | OS | 20/32 | ERM |
| 6 | 54 | M | OD | 20/400 | ERM following macular hole repair |